

MASS-TRANSFER EFFECTS ON HIGHER-ORDER BOUNDARY LAYER SOLUTIONS: THE LEADING EDGE OF A SWEEPED CYLINDER

K. GERSTEN

The Rand Corporation, Santa Monica, California, U.S.A.
and

Professor of Fluid Mechanics, Ruhr University, Bochum, Federal Republic of Germany
and

J. F. GROSS

The Rand Corporation, Santa Monica, California, U.S.A.

(Received 27 December 1971 and in revised form 7 April 1972)

Abstract—The three-dimensional incompressible flow near the stagnation line of a swept cylindrical surface is studied. The method of matched asymptotic expansions is used to obtain an extension of the solutions of the Prandtl boundary-layer equations, i.e. a second approximation to the full Navier–Stokes equations. The second-order effects due to surface curvature and displacement on the velocity components, pressure, shear stress, heat transfer, and mass transfer are determined.

It is shown that the effects of longitudinal curvature and displacement are negative; i.e. they lead to decreasing values of the boundary-layer characteristics: wall shear, heat transfer, and mass transfer. This behavior results from the stretching of the boundary layer normal to the wall by centrifugal forces due to the convex surface curvature. Increasing mass injection at the wall increases all second-order effects. This results from the thickening in the boundary layer produced by injection. Only the curvature effect on wall concentration exhibits the opposite behavior. It increases the wall concentration and this increase is diminished by injection.

NOMENCLATURE

a/b ,	thickness ratio of ellipse [see equation (25b)];	$g(\eta)$	} functions defined in equation (31);	
C ,	species concentration;	$G_c(\eta)$		
C_1, C_2 ,	dimensionless concentration functions, defined in equation (10);	$G_d(\eta)$		
$c(\eta)$	} functions defined in equation (32);	$h(\eta)$	} functions defined in equation (29);	
$C_c(\eta)$		$H_c(\eta)$		
$C_d(\eta)$		$H_d(\eta)$		
C_{ic}, C_{id}	coefficients defined in equations (67)–(72), $i = 1, 2, \dots, 6$;	k ,	} thermal conductivity;	
C_m	mass-transfer parameter defined in equation (38);	Le ,		} Lewis number = Sc/Pr ;
$f(\eta)$	} functions defined in equation (28);	\dot{m} ,		
$F_c(\eta)$		$p(\eta)$	} functions defined in equation (30);	
$F_d(\eta)$		$P_c(\eta)$		
	$P_d(\eta)$	} dimensionless pressure functions defined in equation (8);		
	P_1, P_2 ,		} Prandtl number;	
		Pr ,		

P_r ,	total head = $p_\infty + (\rho/2)U_\infty^2$;	ρ ,	density;
\dot{q} ,	heat transfer [see equation (79a)];	τ ,	shear stress at the wall;
R ,	radius of curvature at the stagnation line (see Fig. 1);	$\bar{\omega}_1, \bar{\omega}_2$,	dimensionless vorticity functions, defined in equations (17) and (19).
Re ,	Reynolds number = $U_\infty R/\nu$;		
Sc ,	Schmidt number;		
T ,	temperature;		
T_1, T_2 ,	dimensionless temperature functions defined in equation (9);	Subscripts	
U_∞ ,	free-stream velocity component perpendicular to the cylinder generators (see Fig. 1);	1,	first-order outer expansion;
U_1, U_2 ,	dimensionless velocity functions defined in equation (7a);	2,	second-order outer expansion;
u ,	velocity component in x -direction;	c ,	surface-curvature effect;
U_{11}, U_{21} ,	constants, defined by equation (24b);	d ,	displacement effect;
V ,	free-stream velocity;	∞ ,	free-stream condition;
V_1, V_2 ,	dimensionless velocity functions defined in equation (7b);	0,	values without second-order effects;
v ,	velocity component in y -direction;	w ,	wall values;
W_∞ ,	free-stream velocity component parallel to the cylinder generators (see Fig. 1);	x ,	longitudinal direction x ;
W_1, W_2 ,	dimensionless velocity functions defined in equation (7c);	z ,	transverse direction z .
x ,	longitudinal coordinate (see Fig. 1);		
\bar{x} ,	dimensionless coordinate = x/R ;		
y ,	coordinate perpendicular to the wall (see Fig. 1);		
\bar{y} ,	dimensionless coordinate = y/R ;		
z ,	coordinate parallel to the cylinder generators.		
Greek symbols			
β_1 ,	constant defined in equation (43a);		
η ,	dimensionless variable of the inner expansion, defined in equation (26);		
κ ,	curvature at the stagnation line = $1/R$;		
ν ,	kinematic viscosity;		
ϕ ,	sweep angle;		

1. INTRODUCTION

PRANDTL'S boundary-layer theory provides a relatively accurate description of a remarkable number of simple flow situations. However, many flows that occur in modern technology possess characteristics that cannot be treated within the simple framework of the Prandtl approximation. It is necessary, for these more complicated flows, to seek approximate solutions to the Navier-Stokes equations that are of higher accuracy than the classical or Prandtl approximation. This extension of classical boundary-layer theory is called higher-order boundary-layer theory, an excellent critical review of which was recently given by Van Dyke [1].

If Prandtl's theory is regarded as the first approximation to the solution of the Navier-Stokes equations, then the retention of terms involving surface curvature and the consideration of the interaction of the boundary layer with special features of the external flow, such as displacement and vorticity, represent the structure upon which the second-order corrections to the Prandtl approximation can be formulated. The method of matched asymptotic expansions is particularly useful in developing

higher approximations to the boundary layer, and Van Dyke has worked out the second-order solutions for incompressible [2, 3] and compressible [4] flows. In fact, higher-order boundary-layer theory has received great attention from many authors, and a comprehensive bibliography may be found in Van Dyke's review.

According to singular perturbation theory, the classical or Prandtl boundary-layer equations are nonlinear, but all the higher-order approximations are linear. Rott and Lenard [5] showed that the second-order correction can be separated into several effects, each associated with a particular physical interpretation. These have been divided into terms representing longitudinal and transverse curvature (terms retained within this order of approximation to the Navier-Stokes equations) and terms associated with the boundary condition at the outer edge of the boundary layer and at the outer flow. These latter effects are due to the displacement of the outer flow by the boundary layer and the varia-

tion of vorticity and stagnation temperature in the outer flow. Other effects, such as the imposition of mass transfer at the surface, three-dimensionality, and the inclusion of a binary gas have not been treated heretofore. We intend to discuss these additional effects for the case of a stagnation line on a swept cylinder. In this study, we restrict ourselves to incompressible flow.

In certain cases of practical interest, the boundary layer may be thickened by viscous heating, transpiration cooling, or ablation. In the case of a body with surface curvature, such as a cylinder, we must include appropriate terms in the solution. In addition to this, even in the absence of vorticity and of variation of stagnation temperature in the outer flow, we must consider the displacement of the outer flow by the boundary layer.

We treat the flow of a binary gas near the stagnation line of a swept cylinder. The free stream is uniconstitutive, with constant velocity V having components $U_\infty = V \cos \phi$ (see Fig.

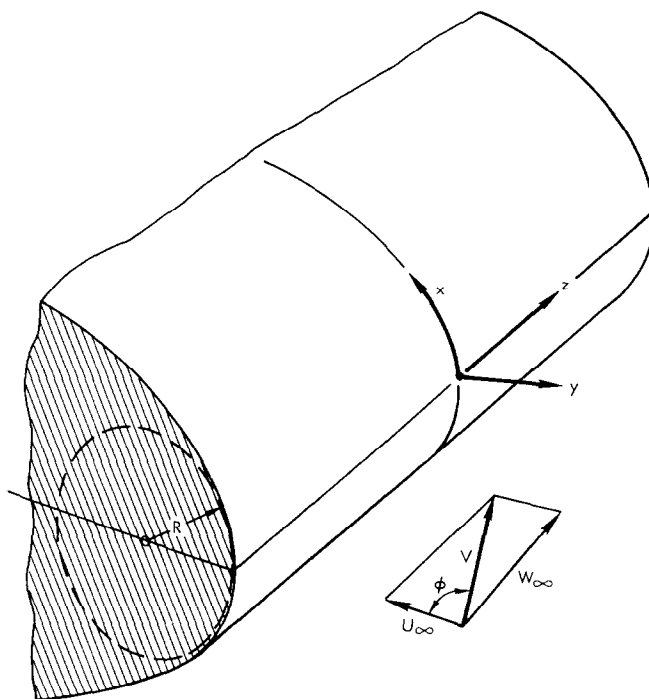


FIG. 1. Coordinate system for the swept cylinder

1) and $W_\infty = V \sin \phi$ (parallel to the generators of the cylinder). A gas is injected at the surface of the cylinder and diffuses through the boundary layer. The method of matched asymptotic expansions is employed to obtain second-order solutions that include the effects of longitudinal curvature and displacement. By "longitudinal curvature" we mean the surface curvature with respect to the flow in the x - y plane. Our solutions will show, to the second order, the effect of mass transfer on wall shear and heat transfer in the three-dimensional boundary layer near the stagnation line of a swept cylinder.

2. GENERAL THEORY

2.1 Basic equations

We begin with the Navier-Stokes equations for an incompressible binary fluid with constant properties. Figure 1 shows the coordinate system for the flow considered here; i.e. the stagnation-line region on a swept cylinder. The velocity components in the x , y and z directions are u , v and w , respectively. The static pressure is p , the temperature is T , and the concentration is given by C . When the free-stream velocity is low and the sweep angle is small, the viscous heating in the energy equation due to the w velocity component may be neglected. In addition, the Schmidt number Sc is taken equal to the Prandtl number, Pr ; i.e. the Lewis number is equal to unity. The equations for steady flow may then be written

$$\begin{aligned} \frac{\partial u}{\partial x} + \frac{\partial}{\partial y}[(1 + \kappa y)v] &= 0 \quad (1) \\ \frac{1}{1 + \kappa y} u \frac{\partial u}{\partial x} + v \frac{\partial u}{\partial y} + \frac{\kappa}{1 + \kappa y} uv + \frac{1}{1 + \kappa y} \frac{1}{\rho} \frac{\partial p}{\partial x} \\ &= v \left[\frac{1}{(1 + \kappa y)^2} \frac{\partial^2 u}{\partial x^2} + \frac{\partial^2 u}{\partial y^2} + \frac{\kappa}{1 + \kappa y} \frac{\partial u}{\partial y} \right. \\ &\quad \left. - \frac{\kappa^2}{(1 + \kappa y)^2} u + \frac{2\kappa}{(1 + \kappa y)^2} \frac{\partial v}{\partial x} \right] \quad (2a) \\ \frac{1}{(1 + \kappa y)} u \frac{\partial v}{\partial x} + v \frac{\partial v}{\partial y} - \frac{\kappa}{1 + \kappa y} u^2 + \frac{1}{\rho} \frac{\partial p}{\partial y} \end{aligned}$$

$$= v \left[\frac{1}{(1 + \kappa y)^2} \frac{\partial^2 v}{\partial x^2} + \frac{\partial^2 v}{\partial y^2} + \frac{\kappa}{1 + \kappa y} \frac{\partial v}{\partial y} - \frac{\kappa^2}{(1 + \kappa y)^2} v - \frac{2\kappa}{(1 + \kappa y)^2} \frac{\partial u}{\partial x} \right] \quad (2b)$$

$$\begin{aligned} \frac{1}{1 + \kappa y} u \frac{\partial w}{\partial x} + v \frac{\partial w}{\partial y} \\ &= v \left[\frac{1}{(1 + \kappa y)^2} \frac{\partial^2 w}{\partial x^2} + \frac{\partial^2 w}{\partial y^2} + \frac{\kappa}{1 + \kappa y} \frac{\partial w}{\partial y} \right] \quad (2c) \end{aligned}$$

$$\begin{aligned} \frac{1}{1 + \kappa y} u \frac{\partial T}{\partial x} + v \frac{\partial T}{\partial y} \\ &= \frac{v}{Pr} \left[\frac{1}{(1 + \kappa y)^2} \frac{\partial^2 T}{\partial x^2} + \frac{\partial^2 T}{\partial y^2} + \frac{\kappa}{1 + \kappa y} \frac{\partial T}{\partial y} \right] \quad (3) \end{aligned}$$

$$\begin{aligned} \frac{1}{1 + \kappa y} u \frac{\partial C}{\partial x} + v \frac{\partial C}{\partial y} \\ &= \frac{v}{Sc} \left[\frac{1}{(1 + \kappa y)^2} \frac{\partial^2 C}{\partial x^2} + \frac{\partial^2 C}{\partial y^2} + \frac{\kappa}{1 + \kappa y} \frac{\partial C}{\partial y} \right]. \quad (4) \end{aligned}$$

Although the flow is independent of z , it is three-dimensional in the sense that it includes the three velocity components. The unknowns in this system of equations are u , v , w , p , T and C . These six equations, together with the appropriate boundary conditions, will be sufficient to obtain a solution.

The boundary conditions for equations (1)–(4) are at the wall ($y = 0$):

$$\left. \begin{aligned} u &= 0 \\ v &= v_w \\ w &= 0 \\ T &= T_w \end{aligned} \right\} \quad (5)$$

far from the body ($y \rightarrow \infty$):

$$\left. \begin{aligned} \sqrt{(u^2 + v^2)} &= U_\infty \\ w &= W_\infty \\ p &= p_\infty \\ T &= T_\infty \\ C &= 0. \end{aligned} \right\} \quad (6)$$

The mass transfer at the wall is given by the boundary conditions for $v = v_w$. It should be noted that, for a binary gas, the Eckert-Schneider condition, which equates the convective flow of a component toward the wall with the diffusive flow away from the wall, links the concentration, the concentration gradient, and the normal velocity at the wall:

$$v_w = -\frac{v}{Sc} \frac{1}{(1 - C_w)} \left(\frac{\partial C}{\partial y} \right)_w \quad (6a)$$

We prescribe the free-stream velocity V , the radius of curvature R , and the sweep angle ϕ , and seek the two components of the wall shear τ_x and τ_z , the heat transfer at the wall \dot{q} , and the mass transfer at the wall \dot{m} , for a given value of the normal wall velocity v_w . The static pressure p_w and the concentration at the wall C_w are not prescribed, but are given by the solution to the equations. The variation of the above quantities with respect to the surface mass transfer will be determined.

2.2 Outer expansions

We nondimensionalize the velocities u and v with a characteristic velocity U_∞ and velocity w with W_∞ . The coordinates are referred to R , the radius of curvature of the cylinder near the stagnation line. The Reynolds number is then given by $U_\infty R/\nu$. The outer expansions of the solutions at high Reynolds number (after Van Dyke [2]) are:

$$\frac{u}{U_\infty} = U_1(\bar{x}, \bar{y}) + \frac{1}{\sqrt{Re}} U_2(\bar{x}, \bar{y}) + \dots \quad (7a)$$

$$\frac{v}{U_\infty} = V_1(\bar{x}, \bar{y}) + \frac{1}{\sqrt{Re}} V_2(\bar{x}, \bar{y}) + \dots \quad (7b)$$

$$\frac{w}{W_\infty} = W_1(\bar{x}, \bar{y}) + \frac{1}{\sqrt{Re}} W_2(\bar{x}, \bar{y}) + \dots \quad (7c)$$

$$\frac{p - p_\infty}{\rho U_\infty^2} = P_1(\bar{x}, \bar{y}) + \frac{1}{\sqrt{Re}} P_2(\bar{x}, \bar{y}) + \dots \quad (8)$$

$$\frac{T}{T_\infty} = T_1(\bar{x}, \bar{y}) + \frac{1}{\sqrt{Re}} T_2(\bar{x}, \bar{y}) + \dots \quad (9)$$

$$C = C_1(\bar{x}, \bar{y}) + \frac{1}{\sqrt{Re}} C_2(\bar{x}, \bar{y}) + \dots \quad (10)$$

Substituting these expressions into equations (1)–(4) and collecting terms of the same order, we obtain for:

the continuity equation:

$$0(1) \quad \frac{\partial U_1}{\partial \bar{x}} + \frac{\partial}{\partial \bar{y}} [(1 + \bar{y}) V_1] = 0 \quad (11a)$$

$$0(1/\sqrt{Re}) \quad \frac{\partial U_2}{\partial \bar{x}} + \frac{\partial}{\partial \bar{y}} [(1 + \bar{y}) V_2] = 0 \quad (11b)$$

velocity u (x-component of momentum equation):

$$0(1) \quad \frac{1}{1 + \bar{y}} U_1 \frac{\partial U_1}{\partial \bar{x}} + V_1 \frac{\partial U_1}{\partial \bar{y}} + \frac{1}{1 + \bar{y}} U_1 V_1 + \frac{1}{1 + \bar{y}} \frac{\partial P_1}{\partial \bar{x}} = 0 \quad (12a)$$

$$0(1/\sqrt{Re}) \quad \frac{1}{1 + \bar{y}} U_2 \frac{\partial U_1}{\partial \bar{x}} + \frac{1}{1 + \bar{y}} U_1 \frac{\partial U_2}{\partial \bar{x}} + V_1 \frac{\partial U_2}{\partial \bar{y}} + V_2 \frac{\partial U_1}{\partial \bar{y}} + \frac{1}{1 + \bar{y}} U_1 V_2 + \frac{1}{1 + \bar{y}} U_2 V_1 + \frac{1}{1 + \bar{y}} \frac{\partial P_2}{\partial \bar{x}} = 0 \quad (12b)$$

velocity v (y-component of momentum equation):

$$0(1) \quad \frac{1}{1 + \bar{y}} U_1 \frac{\partial V_1}{\partial \bar{x}} + V_1 \frac{\partial V_1}{\partial \bar{y}} - \frac{1}{1 + \bar{y}} U_1^2 + \frac{\partial P_1}{\partial \bar{y}} = 0 \quad (13a)$$

$$0(1/\sqrt{Re}) \quad \frac{1}{1 + \bar{y}} U_2 \frac{\partial V_1}{\partial \bar{x}} + \frac{1}{1 + \bar{y}} U_1 \frac{\partial V_2}{\partial \bar{x}} + V_1 \frac{\partial V_2}{\partial \bar{y}} + V_2 \frac{\partial V_1}{\partial \bar{y}} - \frac{2}{1 + \bar{y}} U_1 U_2 + \frac{\partial P_2}{\partial \bar{y}} = 0 \quad (13b)$$

velocity w (z-component of momentum

equation):

$$O(1) \quad \frac{1}{1+\bar{y}} U_1 \frac{\partial W_1}{\partial \bar{x}} + V_1 \frac{\partial W_1}{\partial \bar{y}} = 0 \quad (14a)$$

$$O(1/\sqrt{Re}) \quad \frac{1}{1+\bar{y}} U_1 \frac{\partial W_2}{\partial \bar{x}} + \frac{1}{1+\bar{y}} U_2 \frac{\partial W_1}{\partial \bar{x}} \\ + V_1 \frac{\partial W_2}{\partial \bar{y}} + V_2 \frac{\partial W_1}{\partial \bar{y}} = 0 \quad (14b)$$

energy equation:

$$O(1) \quad \frac{1}{1+\bar{y}} U_1 \frac{\partial T_1}{\partial \bar{x}} + V_1 \frac{\partial T_1}{\partial \bar{y}} = 0 \quad (15a)$$

$$O(1/\sqrt{Re}) \quad \frac{1}{1+\bar{y}} U_1 \frac{\partial T_2}{\partial \bar{x}} + \frac{1}{1+\bar{y}} U_2 \frac{\partial T_1}{\partial \bar{x}} \\ + V_1 \frac{\partial T_2}{\partial \bar{y}} + V_2 \frac{\partial T_1}{\partial \bar{y}} = 0 \quad (15b)$$

concentration equation:

$$O(1) \quad \frac{1}{1+\bar{y}} U_1 \frac{\partial C_1}{\partial \bar{x}} + V_1 \frac{\partial C_1}{\partial \bar{y}} = 0 \quad (16a)$$

$$O(1/\sqrt{Re}) \quad \frac{1}{1+\bar{y}} U_1 \frac{\partial C_2}{\partial \bar{x}} + \frac{1}{1+\bar{y}} U_2 \frac{\partial C_1}{\partial \bar{x}} \\ + V_1 \frac{\partial C_2}{\partial \bar{y}} + V_2 \frac{\partial C_1}{\partial \bar{y}} = 0. \quad (16b)$$

We can eliminate P_1 from equations (12a) and (13a) and show that the nondimensional vorticity

$$\bar{\omega}_1 = \frac{1}{1+\bar{y}} \frac{\partial V_1}{\partial \bar{x}} - \frac{\partial U_1}{\partial \bar{y}} - \frac{1}{1+\bar{y}} U_1 \quad (17a)$$

is constant. Since the vorticity in the free stream is zero, we have

$$\bar{\omega}_1 = 0. \quad (17b)$$

The first-order outer expansion has zero vorticity, and hence is a potential flow. Equations (12a) and (13a), together with equation (17b) yield

$$P_1 + \frac{1}{2}(U_1^2 + V_1^2) = \text{constant} = \frac{1}{2} \quad (18)$$

which is identical to Bernoulli's equation.

Equation (18) defines the pressure P_1 when U_1 and V_1 are known. In a similar manner it can be shown, using equations (11b), (12b) and (13b), that

$$\bar{\omega}_2 = \frac{1}{1+\bar{y}} \frac{\partial V_2}{\partial \bar{x}} - \frac{\partial U_2}{\partial \bar{y}} - \frac{1}{1+\bar{y}} U_2 = 0 \quad (19)$$

and an equation analogous to equation (18) can be derived:

$$P_2 + U_1 U_2 + V_1 V_2 = 0. \quad (20)$$

Imposition of the free-stream conditions on the remaining equations yields the following set of solutions for the components of the transverse velocity w , the temperature T , and the concentration C :

$$\left. \begin{aligned} W_1 &= \text{constant} = 1 \\ W_2 &= \text{constant} = 0 \\ T_1 &= \text{constant} = 1 \\ T_2 &= \text{constant} = 0 \\ C_1 &= \text{constant} = 0 \\ C_2 &= \text{constant} = 0. \end{aligned} \right\} \quad (21)$$

The boundary conditions at the wall for the outer expansions are obtained through matching with the inner expansions. As we will show later [equations (57a) and (57b)], the expressions for $V_1(\bar{x}, 0)$ and $V_2(\bar{x}, 0)$ are given by

$$V_1(\bar{x}, 0) = 0 \quad (22a)$$

$$V_2(\bar{x}, 0) = \sqrt{(U_{11})\beta_1} \quad (22b)$$

where U_{11} and β_1 are constants defined in equations (24b) and (43a). Far from the surface of the cylinder,

$$U_1^2 + V_1^2 = 0 \quad (23a)$$

$$U_2 = 0, \quad V_2 = 0 \quad (23b)$$

where U_1 and V_1 are the velocity components of the potential flow around the body for the case of the solid surface and U_2 and V_2 are the components of the potential flow when $V_2(\bar{x}, 0) \neq 0$.

In dimensionless form, equation (7a) gives the solution for u near the wall as

$$\frac{u(\bar{x}, 0)}{U_\infty} = U_{11}(\bar{x}, 0) + \frac{1}{\sqrt{Re}} U_{21}(\bar{x}, 0) + \dots \quad (24a)$$

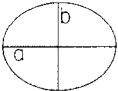
which we write as an expansion for small values of x :

$$\frac{u(\bar{x}, 0)}{U_\infty} = U_{11} \frac{x}{R} + \frac{1}{\sqrt{Re}} U_{21} \frac{x}{R} + \dots \quad (24b)$$

$$= U_{11} \frac{x}{R} \left[1 + \frac{U_{21}}{U_{11}} \frac{1}{\sqrt{Re}} + \dots \right]. \quad (24c)$$

The coefficient for the first-order velocity, U_{11} , is a constant which depends only on the geometry of the body. The following are values of U_{11} for a series of simple shapes:

circular cylinder $U_{11} = 2$ (25a)

ellipse  $U_{11} = 1 + a/b$ (25b)

parabola $U_{11} = 1$ (25c)

thin symmetric Joukowski airfoil $U_{11} = 1$ (25d)

Rankine half body $U_{11} = 1.5$ (25e)

The coefficient for the second approximation, U_{21} , is also a constant which depends only on the displacement speed, i.e. on the growth of the first-order inner solution. There are two values for U_{21} available in the literature. Van Dyke [7] calculated the value for a parabola to be $U_{21} = -0.61$. For the Rankine half body, Devan [8] obtained $U_{21} = -0.62$. Generally one can expect that U_{21} will be negative.

2.3 Inner expansions

The inner expansions are written in the inner variable

$$\eta = \frac{y}{R} \sqrt{(U_{11} Re)}. \quad (26)$$

The following expressions are so formulated that the continuity equation is automatically satisfied. The first term in each case is the first approximation and the last two terms represent the second approximation. The first of these latter two terms is the longitudinal curvature

term, and the second is the displacement-effect term. We write the inner expansions as follows:

$$\frac{u}{U_\infty} = U_{11} \frac{x}{R} \left[f'(\eta) + \frac{1}{\sqrt{(U_{11} Re)}} F'_c(\eta) + \frac{U_{21}}{U_{11}} \frac{1}{\sqrt{Re}} F'_d(\eta) + \dots \right] \quad (27)$$

$$\frac{v}{U_\infty} = \frac{-1}{1 + \frac{\eta}{\sqrt{(U_{11} Re)}}} \frac{\sqrt{(U_{11})}}{\sqrt{Re}} \left[f(\eta) + \frac{1}{\sqrt{(U_{11} Re)}} F_c(\eta) + \frac{U_{21}}{U_{11}} \frac{1}{\sqrt{Re}} F_d(\eta) + \dots \right] \quad (28)$$

$$\frac{w}{W_\infty} = h(\eta) + \frac{1}{\sqrt{(U_{11} Re)}} H_c(\eta) + \frac{U_{21}}{U_{11}} \frac{1}{\sqrt{Re}} H_d(\eta) + \dots \quad (29)$$

$$\frac{p - p_\infty}{\rho U_\infty^2} = \frac{1}{2} - \frac{1}{2} U_{11}^2 \left(\frac{x}{R} \right)^2 \left[p(\eta) + \frac{1}{\sqrt{(U_{11} Re)}} P_c(\eta) + \frac{U_{21}}{U_{11}} \frac{1}{\sqrt{Re}} P_d(\eta) + \dots \right] \quad (30)$$

$$\frac{T - T_w}{T_\infty - T_w} = g(\eta) + \frac{1}{\sqrt{(U_{11} Re)}} G_c(\eta) + \frac{U_{21}}{U_{11}} \frac{1}{\sqrt{Re}} G_d(\eta) \dots \quad (31)$$

$$\frac{C_w - C}{C_w} = c(\eta) + \frac{1}{\sqrt{(U_{11} Re)}} C_c(\eta) + \frac{U_{21}}{U_{11}} \frac{1}{\sqrt{Re}} C_d(\eta) + \dots \quad (32)$$

These expressions can be substituted into the Navier-Stokes equations [equations (1)-(4)] and terms of the same order again collected. In each case, the first equation represents the first approximation of unit order, the second is composed of terms of order $1/\sqrt{Re}$ proportional to U_{11} , and the third consists of terms of order $1/\sqrt{Re}$ proportional to U_{21} .

The equations for u are

$$f''' + ff'' + p - f'^2 = 0 \quad (33a)$$

$$F_c'' + fF_c'' - 2f'F_c' + f''F_c = -P_c - \eta f''' - f'' - ff' \quad (33b)$$

$$F_d'' + fF_d'' - 2f'F_d' + f''F_d = -P_d \quad (33c)$$

The equations for w are

$$h' + fh' = 0 \quad (34a)$$

$$H_c' + fH_c' = (\eta f - 1 - F_c)h' \quad (34b)$$

$$H_d' + fH_d' = -F_d h' \quad (34c)$$

The equations for p are

$$p' = 0 \quad (35a)$$

$$P_c = -2f'^2 \quad (35b)$$

$$P_d = 0 \quad (35c)$$

The equations for T are

$$\frac{1}{Pr} g'' + fg' = 0 \quad (36a)$$

$$\frac{1}{Pr} G_c'' + fG_c' = \left(\eta f - \frac{1}{Pr} - F_c \right) g' \quad (36b)$$

$$\frac{1}{Pr} G_d'' + fG_d' = -F_d g' \quad (36c)$$

The equations for C are

$$\frac{1}{Sc} c'' + fc' = 0 \quad (37a)$$

$$\frac{1}{Sc} C_c'' + fC_c' = \left(\eta f - \frac{1}{Sc} F_c \right) c' \quad (37b)$$

$$\frac{1}{Sc} C_d'' + fC_d' = -F_d c' \quad (37c)$$

The boundary conditions for the foregoing equations are listed below. These values are obtained by direct matching, as shown in the next section, but are given here to complete the problem statement of the system of equations to be solved.

$$\begin{array}{l} f = f_w = -\frac{v_w}{U_\infty} \frac{\sqrt{Re}}{\sqrt{(U_{11})}} = C_m \\ F_c = 0 \\ F_d = 0 \end{array} \quad \begin{array}{l} \eta = 0 \\ F_c' = 0 \\ F_d' = 0 \end{array} \quad \begin{array}{l} \eta \rightarrow \infty \\ f' = 1 \\ F_c'' = -1 \\ F_d' = 1 \end{array} \quad (38)$$

$$\begin{array}{l} h = 0 \\ H_c = 0 \\ H_d = 0 \end{array} \quad \begin{array}{l} h = 1 \\ H_c = 0 \\ H_d = 0 \end{array} \quad (39)$$

$$\begin{array}{l} g = 0 \\ G_c = 0 \\ G_d = 0 \end{array} \quad \begin{array}{l} p = 1 \\ P_c = -2\eta \\ P_d = 2 \end{array} \quad (40)$$

$$\begin{array}{l} g = 0 \\ G_c = 0 \\ G_d = 0 \end{array} \quad \begin{array}{l} g = 1 \\ G_c = 0 \\ G_d = 0 \end{array} \quad (41)$$

$$\left. \begin{aligned} \eta = 0 \\ c = 0 \\ C_c = 0 \\ C_d = 0. \end{aligned} \right\} \quad \left. \begin{aligned} \eta = \infty \\ c = 1 \\ C_c = 0 \\ C_d = 0. \end{aligned} \right\} \quad (42)$$

We obtain the following analytical solutions of equation (35) by using the boundary conditions [equations (38) and (40)] and equation (33a);

$$p = 1$$

$$P_1 = -\beta_1 - \eta - f'' - ff' \quad (43)$$

$$P_2 = 2$$

where

$$\beta_1 = \lim_{\eta \rightarrow \infty} (\eta - f). \quad (43a)$$

2.4 Asymptotic matching

We adopt here the asymptotic matching procedures outlined by Van Dyke [6], whereby the outer expansion in the limit as $\bar{y} \rightarrow 0$ is matched to the inner expansion as $\eta \rightarrow \infty$. For the velocity component u , this procedure yields

$$\begin{aligned} \frac{u}{U_\infty} &= \lim_{\bar{y} \rightarrow 0} \left[U_1(\bar{x}, \bar{y}) + \frac{1}{\sqrt{Re}} U_2(\bar{x}, \bar{y}) \right] \\ &= \lim_{\eta \rightarrow \infty} \left\{ U_{11} \frac{x}{R} \left[f'(\eta) + \frac{1}{\sqrt{(U_{11} Re)}} F'_c(\eta) \right. \right. \\ &\quad \left. \left. + \frac{U_{21}}{U_{11}} \frac{1}{\sqrt{Re}} F'_d(\eta) \right] \right\}. \quad (44)
 \end{aligned}$$

The outer flow can be expanded for small \bar{y} in a Taylor's series:

$$\begin{aligned} \lim_{\bar{y} \rightarrow 0} U_1(\bar{x}, \bar{y}) &= U_1(\bar{x}, 0) \\ &+ \bar{y} \left(\frac{\partial U_1}{\partial \bar{y}} \right)_w + O(\bar{y}^2). \quad (45)
 \end{aligned}$$

Since $\bar{\omega}_1 = 0$, we can write according to equation (17)

$$\begin{aligned} \left(\frac{\partial U_1}{\partial \bar{y}} \right)_w &= - \left(\frac{1}{1 + \bar{y}} U_1 \right)_w + \left(\frac{1}{1 + \bar{y}} \frac{\partial V_1}{\partial \bar{x}} \right)_w \\ &= -U_1(\bar{x}, 0) + \left(\frac{\partial V_1}{\partial \bar{x}} \right)_w. \quad (46)
 \end{aligned}$$

Then

$$\begin{aligned} \lim_{\bar{y} \rightarrow 0} U_1(\bar{x}, \bar{y}) &= U_1(\bar{x}, 0) [1 - \bar{y}] \\ &+ \bar{y} \left(\frac{\partial V_1}{\partial \bar{x}} \right)_w + O(\bar{y}^2)
 \end{aligned}$$

or, for small \bar{x}

$$\begin{aligned} \lim_{\bar{y} \rightarrow 0} U_1(\bar{x}, \bar{y}) &= U_{11} \frac{x}{R} [1 - \bar{y}] \\ &+ \bar{y} \left(\frac{\partial V_1}{\partial \bar{x}} \right)_w + O(\bar{y}^2). \quad (47)
 \end{aligned}$$

Similarly, it can be shown that

$$\begin{aligned} \lim_{\bar{y} \rightarrow 0} U_2(\bar{x}, \bar{y}) &= U_{21} \frac{x}{R} [1 - \bar{y}] \\ &+ \bar{y} \left(\frac{\partial V_2}{\partial \bar{x}} \right)_w + O(\bar{y}^2). \quad (48)
 \end{aligned}$$

Then we may write equation (44) as:

$$\begin{aligned} &U_{11} \frac{x}{R} [1 - \bar{y}] + \bar{y} \left(\frac{\partial V_1}{\partial \bar{x}} \right)_w + \frac{1}{\sqrt{Re}} U_{21} \\ &\times \frac{x}{R} [1 - \bar{y}] + \frac{1}{\sqrt{Re}} \bar{y} \left(\frac{\partial V_2}{\partial \bar{x}} \right)_w + O(\bar{y}^2) \\ &= \lim_{\eta \rightarrow \infty} \left\{ U_{11} \frac{x}{R} \left[f'(\eta) + \frac{1}{\sqrt{(U_{11} Re)}} F'_c(\eta) \right. \right. \\ &\quad \left. \left. + \frac{U_{21}}{U_{11}} \frac{1}{\sqrt{Re}} F'_d(\eta) \right] \right\}. \quad (49)
 \end{aligned}$$

Noting that $\bar{y} = \eta / \sqrt{(U_{11} Re)}$, we obtain from the matching

$$\lim_{\eta \rightarrow \infty} f'(\eta) = 1 \quad (50a)$$

$$\lim_{\eta \rightarrow \infty} F'_c(\eta) = -\eta \quad (50b)$$

$$\lim_{\eta \rightarrow \infty} F'_d(\eta) = 1. \quad (50c)$$

The normal velocity v may be written

$$\begin{aligned} \frac{v}{U_\infty} &= \lim_{\bar{y} \rightarrow 0} \left[V_1(\bar{x}, \bar{y}) + \frac{1}{\sqrt{Re}} V_2(\bar{x}, \bar{y}) \right] \\ &= \lim_{\eta \rightarrow \infty} \left\{ -\frac{U_{11}}{\sqrt{(U_{11} Re)}} \right. \\ &\quad \left. \left[f(\eta) + O\left(\frac{1}{\sqrt{(U_{11} Re)}}\right) \right] \right\}. \end{aligned} \quad (51)$$

Both V_1 and V_2 are expanded for small \bar{y} :

$$\lim_{\bar{y} \rightarrow 0} V_1(\bar{x}, \bar{y}) = V_1(\bar{x}, 0) + \bar{y} \left(\frac{\partial V_1}{\partial \bar{y}} \right)_w + O(\bar{y}^2) \quad (52)$$

$$\lim_{\bar{y} \rightarrow 0} V_2(\bar{x}, \bar{y}) = V_2(\bar{x}, 0) + \bar{y} \left(\frac{\partial V_2}{\partial \bar{y}} \right)_w + O(\bar{y}^2). \quad (53)$$

The continuity equation yields the following expressions for the derivatives of V_1 and V_2 at $\bar{y} \rightarrow 0$ and small values of \bar{x} :

$$\begin{aligned} \left(\frac{\partial V_1}{\partial \bar{y}} \right)_w &= -V_1(\bar{x}, 0) - \left(\frac{\partial U_1}{\partial \bar{x}} \right)_w \\ &= -V_1(\bar{x}, 0) - U_{11} \end{aligned} \quad (54)$$

$$\begin{aligned} \left(\frac{\partial V_2}{\partial \bar{y}} \right)_w &= -V_2(\bar{x}, 0) - \left(\frac{\partial U_2}{\partial \bar{x}} \right)_w \\ &= -V_2(\bar{x}, 0) - U_{21}. \end{aligned} \quad (55)$$

Equating the expressions for v gives:

$$\begin{aligned} &V_1(\bar{x}, 0) - \bar{y} V_1(\bar{x}, 0) - \bar{y} U_{11} \\ &+ \frac{1}{\sqrt{Re}} V_2(\bar{x}, 0) - \frac{\bar{y}}{\sqrt{Re}} V_2(\bar{x}, 0) \\ &- \frac{\bar{y}}{\sqrt{Re}} U_{21} + O(\bar{y}^2) \\ &= \lim_{\eta \rightarrow \infty} \left\{ -\frac{U_{11}}{\sqrt{(U_{11} Re)}} f(\eta) + O\left(\frac{1}{\sqrt{(U_{11} Re)}}\right) \right\}. \end{aligned} \quad (56)$$

The matching procedure for v yields:

$$V_1(\bar{x}, 0) = 0 \quad (57a)$$

$$\begin{aligned} V_2(\bar{x}, 0) &= \sqrt{(U_{11})} \left[\lim_{\eta \rightarrow \infty} (\eta - f) \right] \\ &= \sqrt{(U_{11})} \beta_1. \end{aligned} \quad (57b)$$

In a similar manner, the inner and outer expansions for the pressure are set equal:

$$\begin{aligned} \frac{p - p_\infty}{\rho U_\infty^2} &= \lim_{\bar{y} \rightarrow 0} \left[P_1(\bar{x}, \bar{y}) + \frac{1}{\sqrt{Re}} P_2(\bar{x}, \bar{y}) \right] \\ &= \lim_{\eta \rightarrow \infty} \left\{ \frac{1}{2} - \frac{1}{2} U_{11}^2 \left(\frac{x}{R} \right)^2 \times \left[p(\eta) + \right. \right. \\ &\quad \left. \left. \frac{1}{\sqrt{(U_{11} Re)}} P_c(\eta) + \frac{U_{21}}{U_{11}} \frac{1}{\sqrt{Re}} P(\eta) \right] \right\}. \end{aligned} \quad (58)$$

The outer-expansion pressure components P_1 and P_2 are expanded in Taylor's series to give

$$\lim_{\bar{y} \rightarrow 0} P_1(\bar{x}, \bar{y}) = P_1(\bar{x}, 0) + \bar{y} \left(\frac{\partial P_1}{\partial \bar{y}} \right)_w + O(\bar{y}^2) \quad (59)$$

$$\lim_{\bar{y} \rightarrow 0} P_2(\bar{x}, \bar{y}) = P_2(\bar{x}, 0) + \bar{y} \left(\frac{\partial P_2}{\partial \bar{y}} \right)_w + O(\bar{y}^2). \quad (60)$$

From equation (18), we obtain:

$$\begin{aligned} \left(\frac{\partial P_1}{\partial \bar{y}} \right)_w &= -U_1(\bar{x}, 0) \left(\frac{\partial U_1}{\partial \bar{y}} \right)_w \\ &\quad - V_1(\bar{x}, 0) \left(\frac{\partial V_1}{\partial \bar{y}} \right)_w \end{aligned} \quad (61)$$

or, by using equation (46)

$$\left(\frac{\partial P_1}{\partial \bar{y}} \right)_w = U_1^2(\bar{x}, 0). \quad (62)$$

Using equations (18) and (20), we obtain P_1 and P_2 for small values of x :

$$\begin{aligned} P_1(\bar{x}, \bar{y}) &= \frac{1}{2} - \frac{1}{2} U_{11}^2 \left(\frac{x}{R} \right)^2 \\ &\quad + U_{11}^2 \left(\frac{x}{R} \right)^2 \bar{y} + O(\bar{y}^2) \end{aligned} \quad (63)$$

$$P_2(\bar{x}, \bar{y}) = -U_{11} U_{21} \left(\frac{x}{R} \right)^2 + O(\bar{y}). \quad (64)$$

The matching procedure then yields:

$$\lim_{\eta \rightarrow \infty} p = 1 \quad (65a)$$

$$\lim_{\eta \rightarrow \infty} P_c = -2\eta \quad (65b)$$

$$\lim_{\eta \rightarrow \infty} P_d = 2. \quad (65c)$$

2.5 Boundary-layer characteristics

The shear stress at the wall in the x -direction can be written

$$\tau_x = \rho v \left(\frac{\partial u}{\partial y} \right)_w = \rho v \frac{x}{R^2} U_\infty U_{11} \sqrt{(U_{11} Re)} \left(f_w'' + \frac{1}{\sqrt{(U_{11} Re)}} F_{cw}'' + \frac{U_{21}}{U_{11}} \frac{1}{\sqrt{Re}} F_{dw}'' \right) \quad (66)$$

where the indices w refer to the values of the functions at the wall $\eta = 0$. When τ_x is normalized by the value that obtains in the absence of second-order effects, τ_{x0} , we get

$$\frac{\tau_x}{\tau_{x0}} = 1 - \frac{1}{\sqrt{(U_{11} Re)}} C_{1c} + \frac{U_{21}}{U_{11} \sqrt{Re}} C_{1d}. \quad (67)$$

The remaining boundary-layer characteristics may be written in a similar manner:

$$\frac{\tau_z}{\tau_{z0}} = 1 - \frac{1}{\sqrt{(U_{11} Re)}} C_{2c} + \frac{U_{21}}{U_{11} \sqrt{Re}} C_{2d} \quad (68)$$

$$\frac{p_t - p_w}{p_t - p_{w0}} = 1 - \frac{1}{\sqrt{(U_{11} Re)}} C_{3c} + \frac{U_{21}}{U_{11} \sqrt{Re}} C_{3d} \quad (69)$$

$$\frac{\dot{q}}{\dot{q}_0} = 1 - \frac{1}{\sqrt{(U_{11} Re)}} C_{4c} + \frac{U_{21}}{U_{11} \sqrt{Re}} C_{4d} \quad (70)$$

$$\frac{\dot{m}}{\dot{m}_0} = 1 - \frac{1}{\sqrt{(U_{11} Re)}} C_{5c} + \frac{U_{21}}{U_{11} \sqrt{Re}} C_{5d} \quad (71)$$

$$\frac{C_w}{C_{w0}} = 1 + \frac{1}{\sqrt{(U_{11} Re)}} C_{6c} + \frac{U_{21}}{U_{11} \sqrt{Re}} C_{6d} \quad (72)$$

where $p_t = p_\infty + (\rho/2)U_\infty^2$ is the total head.

The values of the second approximation coefficients C_{1c} to C_{6c} , C_{1d} to C_{6d} are positive, and are given by

$$C_{1c} = -\frac{F_{cw}''}{f_w''} \quad C_{1d} = \frac{F_{dw}''}{f_w''} \quad (73)$$

$$C_{2c} = -\frac{H'_{cw}}{h'_w} \quad C_{2d} = \frac{H'_{dw}}{h'_w} \quad (74)$$

$$C_{3c} = -P_{cw} = \beta_1 + f_w'' \quad C_{3d} = P_{dw} = 2 \quad (75)$$

$$C_{4c} = -\frac{G'_{cw}}{g'_w} \quad C_{4d} = \frac{G'_{dw}}{g'_w} \quad (76)$$

$$C_{5c} = -\frac{C'_{cw}}{c'_w} \quad C_{5d} = \frac{C'_{dw}}{c'_w} \quad (77)$$

$$C_{6c} = \frac{C'_{cw}}{f_w Sc - c'_w} \quad C_{6d} = -\frac{C'_{dw}}{f_w Sc - c'_w}. \quad (78)$$

The heat transfer, \dot{q} , and the mass transfer, \dot{m} , are defined in the usual way by the gradients of temperature and concentration at the wall:

$$\dot{q} = -k \left(\frac{\partial T}{\partial y} \right)_w \quad (79a)$$

$$\dot{m} = -\frac{v}{Sc} \left(\frac{\partial C}{\partial y} \right)_w = (1 - C_w) v_w. \quad (79b)$$

The concentration at the wall is determined by the Eckert-Schneider condition, equation (6a). For the case without second-order effects, we get

$$C_{w0} = \frac{f_w Sc}{f_w Sc - c'_w}. \quad (80)$$

From equations (79) and (80), it can be seen that \dot{m} and C_{w0} are equal to zero for $v_w = 0$ ($f_w = 0$). This is the case for no mass transfer; the ratios \dot{m}/\dot{m}_0 and C_w/C_{w0} , however, have finite values.

3. RESULTS AND DISCUSSION

We have determined the second approximation to the solution of the Navier-Stokes equations for incompressible, three-dimensional flow in the neighborhood of a stagnation line on a swept cylinder.

We used the methods of matched asymptotic expansions to determine the coefficients in expansions for the flow velocity components, pressure, temperature, cross flow at the wall, and wall concentration. In this way, we studied the effect of wall mass transfer on the second approximation coefficients for longitudinal

curvature and displacement. In addition, we obtained a first approximation to the three-dimensional flow by introducing a sweep angle in the flow which brings in the transverse velocity, w . It should be noted that this velocity, as well as all the other boundary-layer characteristics, are independent of z .

The results of the matching procedure and the numerical calculations are given in equations (67)–(80), which present the numerical coefficients for the second approximation in longitudinal curvature and displacement. The numerical values of all functions at the wall are listed in Table 1. Since the Reynolds number contains $U_\infty = V \cos \phi$, the effect of the sweep angle can be obtained directly. Since all coefficients in equations (67)–(72) are positive, the direction of the second-order effects on the boundary-layer characteristics can be seen from the signs preceding the coefficients. If we assume that U_{21} is negative, as indicated above, then all of the second-order effects are negative, i.e. lead to decreasing values of the characteristics. The sole exception is the longitudinal curvature effect on the wall concentration. This reduction reflects the increase in thickness of the boundary layer due to centrifugal forces resulting from the convex wall curvature. The reduction of $p_t - p_w$ means an increase in the value of the wall pressure p_w with respect to the inviscid value p_{w0} . The explanation is as follows. In the inviscid solution, the pressure gradient perpendicular to the wall is present because of the convex curvature of the wall. This pressure gradient at the wall is positive because of the streamline curvature near the wall. When viscous forces are taken into account, the centrifugal forces near the wall are reduced, and hence also is the pressure gradient. Since the matching condition with the outer flow remains the same, the pressure at the wall must increase.

All the coefficients in equations (67)–(72), with the exception of C_{3d} , are dependent on the mass-transfer parameter

$$C_m = f_w = -\frac{v_w}{U_\infty} \frac{\sqrt{Re}}{\sqrt{(U_{11})}} \quad (81)$$

Figures 2–4 show the variation of the second approximation coefficients with wall mass transfer, C_m , for suction and injection. Figure 2 shows

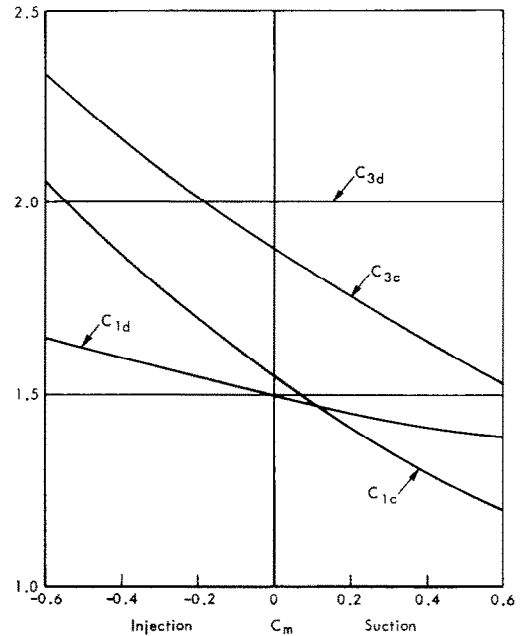


FIG. 2. Effect of mass transfer on the second approximation coefficients for longitudinal curvature and displacement [see equations (67) and (69)].

the variation of longitudinal shear stress and wall pressure. Transverse wall shear stress, heat transfer ($Pr = 0.7$), and mass transfer ($Sc = 0.7$) at the wall are plotted in Fig. 3. Finally, Fig. 4 shows the coefficients for the concentration at the wall. The absolute values of the coefficients given in Fig. 2 are about an order of magnitude greater than those in Fig. 3, but their range of relative variation with respect to mass transfer is much less. The values shown in Fig. 4 have the same order of magnitude as in Fig. 3, but exhibit much less relative variation with mass transfer.

Inspection of Figs. 2 and 3 show that increasing mass transfer increases all second approximation coefficients. This results from the increase in boundary-layer thickness due to injection. Since the second-order curvature effects are proportional to δ/R , it is clear that

Table 1. Functions of the inner expansion: numerical values at the wall

f_w	f_w^*	β_1^*	F_{ew}''	β_c^\dagger	F_{dw}''	β_d^\ddagger	h_w	H_{ew}'	H_{dw}'	$g_w' = g_w'$ ($Pr = Sc = 0.7$)	$G_{ew}' = G_{ew}'$ ($Pr = Sc = 0.7$)	$G_{dw}' = G_{dw}'$ ($Pr = Sc = 0.7$)
0.5	1.54175	0.04233	-1.93130	0.52455	2.14779	0.31789	0.92176	-0.13020	0.27069	0.74099	-0.10436	0.23947
0.4	1.47660	0.16148	-1.92812	0.56046	2.08616	0.31996	0.84671	-0.13654	0.27539	0.68919	-0.10915	0.24226
0.3	1.41304	0.28157	-1.92475	0.59942	2.02545	0.32165	0.77386	-0.14283	0.27938	0.63868	-0.11398	0.24459
0.2	1.35114	0.40264	-1.92117	0.64168	1.96567	0.32290	0.70339	-0.14896	0.28249	0.58955	-0.11879	0.24638
0.1	1.29097	0.52474	-1.91734	0.68739	1.90682	0.32368	0.63552	-0.15480	0.28451	0.54191	-0.12353	0.24753
0	1.23259	0.64790	-1.91324	0.73656	1.84888	0.32393	0.57047	-0.16018	0.28523	0.49587	-0.12811	0.24793
-0.1	1.17604	0.77217	-1.90886	0.78965	1.79187	0.32362	0.50845	-0.16491	0.28444	0.45152	-0.13245	0.24749
-0.2	1.12139	0.89758	-1.90432	0.85278	1.73577	0.32271	0.44969	-0.16882	0.28190	0.40898	-0.13646	0.24608
-0.3	1.06867	1.02416	-1.89924	0.91363	1.68060	0.32083	0.39439	-0.17161	0.27743	0.36837	-0.13997	0.24361
-0.4	1.01794	1.15195	-1.89426	1.00743	1.62637	0.31827	0.34277	-0.17317	0.27085	0.32978	-0.14296	0.23997
-0.5	0.96923	1.28096	-1.88852	1.09793	1.57308	0.31367	0.29498	-0.17313	0.26204	0.29332	-0.14517	0.23507

* $\beta_1 = \lim_{\eta \rightarrow \infty} (\eta - f)$.

† $\beta_c = \lim_{\eta \rightarrow \infty} (\eta^2, 2 + F_c)$.

‡ $\beta_d = \lim_{\eta \rightarrow \infty} (\eta - F_d)$.

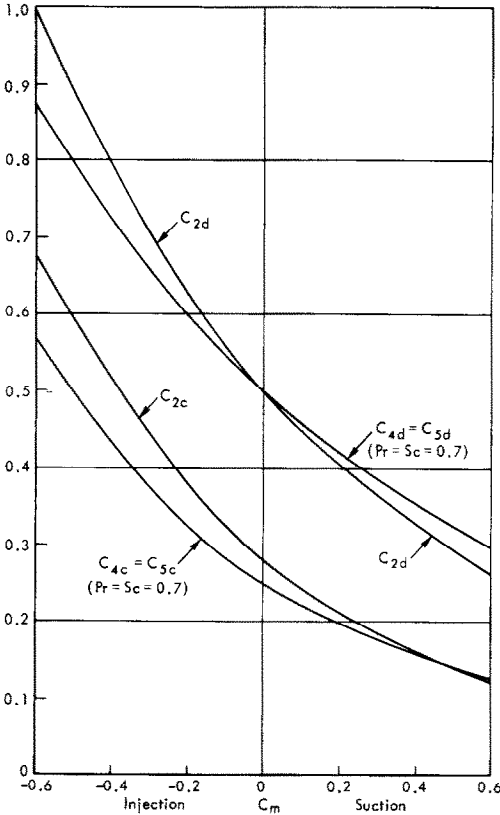


FIG. 3. Effect of mass transfer on the second approximation coefficients for curvature and displacement [see equations (68), (70) and (71)].

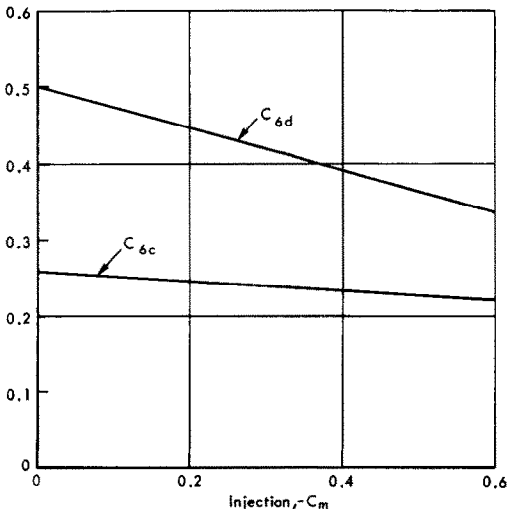


FIG. 4. Effect of mass transfer on the second approximation coefficients for curvature and displacement [see equation (72)].

they will increase with injection. Second-order effects due to displacement obviously will show the same dependence on mass injection as does surface curvature. Increasing the boundary-layer thickness will result in greater displacement effects.

Figure 4 shows that coefficients for the wall concentration exhibit the opposite tendency; i.e. they decrease slightly with increasing wall mass injection. The concentration is obtained from the Eckert-Schneider condition, and the tendency for the coefficients to decrease indicates that the increase due to the first-order wall concentration is greater than that contributed by the additional terms due to second-order effects. The coefficients for $C_m = 0$ in this report are identical with those found by Van Dyke [3].

It must be re-emphasized here that the calculation of the coefficient U_{21} , which determines the magnitude of the displacement effect at the stagnation point, involves the global solution to the potential flow over the effective body, which consists of a boundary layer and an airfoil. This calculation has been performed by Van Dyke for a semi-finite body (parabola), and by Devan for the Rankine body. For the case of a closed body, however, it is not at all clear just how the coefficient can be determined, since the wake and the separation region can have a considerable effect on the effective body shape because of body and viscous layers.

REFERENCES

1. M. VAN DYKE, *Ann. Rev. Fluid Mech.* **1**, 265 (1969).
2. M. VAN DYKE, *J. Fluid Mech.* **14**, 161 (1962).
3. M. VAN DYKE, *J. Fluid Mech.* **14**, 481 (1962).
4. M. VAN DYKE, *Hypersonic Flow Research*, edited by F. R. RIDELL, p. 37. Academic Press, New York (1962).
5. N. ROTT and M. LENARD, *J. Aerospace Sci.* **26**, 542 (1959).
6. M. VAN DYKE, *Perturbation Methods in Fluid Mechanics*. Academic Press, New York (1964).
7. M. VAN DYKE, *J. Fluid Mech.* **19**, 145 (1964).
8. L. DEVAN, Second order incompressible laminar boundary layer development on a two-dimensional semi-infinite body. Ph.D. Thesis, University of California at Los Angeles (1964).

EFFETS DU TRANSFERT MASSIQUE SUR LES SOLUTIONS D'ORDRE ELEVE DE
LA COUCHE LIMITE: BORD D'ATTAQUE D'UN CYLINDRE

Résumé— On étudie l'écoulement incompressible tridimensionnel près de la ligne d'arrêt d'une surface cylindrique. La méthode du développement asymptotique est utilisée pour obtenir une extension des solutions des équations de la couche limite de Prandtl, par exemple la seconde approximation des équations complètes de Navier–Stokes. On détermine les effets de second ordre dus à la courbure de la surface et au déplacement sur les composantes de la vitesse, sur la pression, la tension tangentielle, le transfert thermique et massique.

On montre que les effets de la courbure longitudinale et du déplacement sont négatifs en entraînant des valeurs décroissantes des caractéristiques de la couche limite: tension tangentielle, transfert thermique et massique. Ce comportement résulte de l'action des forces centrifuges dues à la convexité de la surface. Une injection massique à la paroi augmente tous les effets du second ordre. Ceci résulte de l'épaississement de la couche limite par l'injection. L'effet de courbure révèle uniquement une influence opposée sur la concentration pariétale. Il augmente la concentration à la paroi et cet accroissement est réduit par l'injection.

MASSENTRANSPORT-EFFEKTE AUF GRENZSCHICHTLÖSUNGEN HÖHERER
ORDNUNG
DIE ANSTRÖMKANTE DES UMSTRÖMTEN ZYLINDERS.

Zusammenfassung—Es wurde die dreidimensionale inkompressible Strömung an der Staulinie einer umströmten zylindrischen Fläche untersucht. Es wurde die Methode der schrittweise asymptotischen Expansion genutzt, um eine Erweiterung der Lösung der Prandtl-schen Grenzschichtgleichungen zu erhalten, d.h. eine zweite Näherung der vollen Navier–Stokes'schen Gleichungen. Es wurden die durch die Oberflächenkontur bedingten Auswirkungen zweiter Ordnung auf die Geschwindigkeitskomponenten, den Druck, die Schubspannung, den Wärme- und den Stoffübergang bestimmt.

Es wurde gezeigt, dass die Krümmung der Oberflächenkontur in Längsrichtung sich vermindern auswirkt, d.h. die Werte charakteristischer Größen in der Grenzschicht nehmen ab: die Wandschubspannung, der Wärme- und der Stoffübergang. Dieses Verhalten ergibt sich durch die Ausbreitung der Grenzschicht normal zur Wand durch Zentrifugalkräfte aufgrund der konvexen Oberflächenkrümmung. Gesteigerte Massenzufuhr an der Wand erhöht alle Effekte zweiter Ordnung. Dies ergibt sich durch die Verdickung der Grenzschicht durch die Massenzufuhr. Nur die Auswirkung der Krümmung auf die Wandkonzentration zeigt ein anderes Verhalten. Sie führt zu einer Erhöhung der Wandkonzentration und diese Erhöhung lässt sich durch Massenzufuhr verringern.

ВЛИЯНИЕ УЧЕТА ПЕРЕНОСА МАССЫ НА РЕЗУЛЬТАТЫ РЕШЕНИЯ
УРАВНЕНИЙ ПОГРАНИЧНОГО СЛОЯ ВЫСОКИХ ПОРЯДКОВ
ОБЛАСТЬ ПЕРЕДНЕЙ КРИТИЧЕСКОЙ ТОЧКИ ПОПЕРЕЧНООПТЕКАЕМОГО
ЦИЛИНДРА

Аннотация—Проведено исследование трехмерного несжимаемого потока вблизи критической точки поперечнооптекаемого цилиндра. Определяется влияние эффектов второго порядка кривизны поверхности и вытеснения на компоненты скорости, давления, напряжения сдвига и тепло-и массообмен.

Показано, что влияние продольной кривизны и вытеснения отрицательно, т.к. оно приводит к уменьшению характеристик пограничного слоя (напряжения, коэффициентов трения). Это происходит в результате утолщения пограничного слоя под воздействием центробежных сил, возникающих из-за того, что поверхность имеет выпуклую конфигурацию. Увеличение вдува на стенке ведет к росту всех эффектов второго порядка, т.к. вдув приводит к увеличению толщины пограничного слоя. Влияние кривизны на концентрацию на стенке противоположно по своему вышеописанному характеру: она увеличивает концентрации, в то время как вдув тормозит это увеличение.